Downloaded from orbit.dtu.dk on: Mar 25, 2025

DTU Library

Autoignition enhancement of methane by admixture of low fraction of acetaldehyde: simulations and RCM experiments in stoichiometric and rich mixtures

Nourani Najafi, S. B. ; Gersen, S.; Hashemi, H.; Glarborg, P.; Mokhov, A.V.; Levinsky, H. B.

Published in:
International Journal of Chemical Kinetics

Link to article, DOI:
10.1002/kin.21727

Publication date:
2024

Document Version
Publisher's PDF, also known as Version of record

Link back to DTU Orbit

Citation (APA):
Nourani Najafi, S. B., Gersen, S., Hashemi, H., Glarborg, P., Mokhov, A. V., & Levinsky, H. B. (2024). Autoignition enhancement of methane by admixture of low fraction of acetaldehyde: simulations and RCM experiments in stoichiometric and rich mixtures. *International Journal of Chemical Kinetics*, *56*(9), 534-548. https://doi.org/10.1002/kin.21727

General rights
Copyright and moral rights for the publications made accessible in the public portal are retained by the authors and/or other copyright owners and it is a condition of accessing publications that users recognise and abide by the legal requirements associated with these rights.

- Users may download and print one copy of any publication from the public portal for the purpose of private study or research.
- You may not further distribute the material or use it for any profit-making activity or commercial gain
- You may freely distribute the URL identifying the publication in the public portal

If you believe that this document breaches copyright please contact us providing details, and we will remove access to the work immediately and investigate your claim.

Check for updates

Received: 26 November 2023 | Revised: 14 March 2024 | Accepted: 10 April 2024

DOI: 10.1002/kin.21727

INTERNATIONAL JOURNAL OF CHEMICAL KINETICS WILEY

RESEARCH ARTICLE

Autoignition enhancement of methane by admixture of low fraction of acetaldehyde: Simulations and RCM experiments in stoichiometric and rich mixtures

Seyed B. Nourani Najafi[1,4] | **Sander Gersen**[2] | **Hamid Hashemi**[3] | **Peter Glarborg**[3] | **Anatoli V. Mokhov**[1] | **Howard B. Levinsky**[1]

[1]Energy Conversion, Energy and Sustainability Research Institute, University of Groningen, Groningen, The Netherlands

[2]DNV Oil & Gas, Nederland B. V. Groningen, Groningen, The Netherlands

[3]Department of Chemical and Biochemical Engineering, Technical University of Denmark, Lyngby, Denmark

[4]HAN Automotive Research, HAN University of Applied Sciences, Ruitenberglaan 29, 6826 CC, Arnhem, The Netherlands

Correspondence
A.V. Mokhov, Energy and Sustainability Research Institute, University of Groningen, Nijenborgh 6, 9747 AG Groningen, The Netherlands.
Email: A.V.Mokhov@rug.nl

Abstract

The effect of small fractions of acetaldehyde (CH_3CHO) on the ignition delay time of methane (CH_4) was examined at high pressure. Measurements are reported for the ignition delay time obtained in a rapid compression machine (RCM) at a compression pressure (P_c) of ~60 bar and temperatures after compression (T_c) in the range 750–900 K for fuel-air equivalence ratios ϕ in the range 1–4. The results show that mixtures of 2%–5% CH_3CHO in CH_4 ignite under conditions at which pure methane does not ignite experimentally. The efficiency of acetaldehyde as a promoter seems to be comparable to that of other oxygenated fuels like alcohols and ethers. For comparison with the experimental results, ignition delay times are computed using an updated reaction mechanism and two mechanisms from the literature for CH_3CHO oxidation. For most conditions, the simulations using the current mechanism agree with the measurements to within a factor of two. The ignition profile shows a pre-ignition temperature rise and two-stage ignition similar to that previously observed in low fractions of dimethyl ether in ammonia; both phenomena are captured by the simulations. Analysis of simulations at constant volume indicates that CH_3CHO is oxidized much more rapidly than CH_4, producing reactive species that initiate the oxidation of CH_4 and generates heat that accelerates oxidation toward ignition. The low-temperature chain-branching reactions of CH_3CHO are important in the early oxidation of the fuel mixture. Additional simulations were performed for equivalence ratios of $\phi = 1$ and 4, at a compression pressure (P_c) of 100 bar and T_c = 750–1000 K. The simulations indicate that CH_3CHO has a strong ignition-enhancing effect on CH_4, with small fractions reducing the ignition delay time by up to a factor of 100, depending on the temperature, as compared to pure CH_4.

This is an open access article under the terms of the Creative Commons Attribution License, which permits use, distribution and reproduction in any medium, provided the original work is properly cited.
© 2024 The Author(s). *International Journal of Chemical Kinetics* published by Wiley Periodicals LLC.

INTERNATIONAL JOURNAL OF CHEMICAL KINETICS WILEY

KEYWORDS
ignition enhancement, methane/acetaldehyde ignition, pre-ignition heat release, RCM measurements

1 | INTRODUCTION

The excellent knock resistance of methane makes natural gas (consisting predominantly of methane) and its renewable replacement, biomethane (e.g., via the anaerobic digestion of biomass[1]), very suitable fuels for spark-ignited (SI) engines.[2] At the same time, this resistance to autoignition under engine conditions excludes its use for engines that rely on compression ignition (CI), such as diesel engines, without the use of a pilot fuel for ignition (see, e.g.,[3]). Adding small quantities of an ignition enhancer to natural gas/biomethane to facilitate CI would permit its use in diesel-type engines, which have significantly higher efficiencies than SI engines. Combined with the potential for reduced methane slip[3] as compared to SI engines, use of methane-based fuels in efficient CI engines can reduce the CO_2 footprint of the utilization of these fuels.

The ignition enhancement of methane by other fuel components has been examined in studies under engine-relevant conditions. A range of different promoters has been investigated in rapid compression machines (RCMs) and shock tubes.[3–9] The ignition properties of methane with various fuels, such as H_2 (e.g., at 10–70 bar and 960–1060 K[6]), higher alkanes, for example, ethane (25–50 bar and 900–1050 K[7]), and diesel fuel (6–20 bar and 640–1450 K[5]), have been reported. Oxygenated species have also been studied, such as dimethyl ether (DME) (60 bar and 700–900 K[3] and 7–41 atm and 600–1600 K in RCM and shock tube[4]), ethanol and *n*-propanol (3–10 atm and 1100–1500 K in a shock tube[9]), and methyl propanoate (4–10 atm and 1000–1500 K in a shock tube[8]). The oxygenated compounds exhibit ignition delay times nearly two orders of magnitude shorter than that of methane and the addition of these fuels substantially decreases the ignition delay time of methane. The mechanism of enhancement is often specific to a given additive. For example, at ~1000 K, the effect of hydrogen has been ascribed[10] to interaction of H_2 in low-temperature reactions of methane, while reactions of DME itself has been shown to control the ignition of methane/DME mixtures.[4] The chemical coupling between methane and additive components is further complicated by the observation that the effect of addition on the ignition delay is often non-linear in additive fraction.[6,8]

Acetaldehyde (CH_3CHO) is a commonly used intermediate in chemical synthesis of industrial chemicals, which can be produced from (bio)ethanol.[11] The heating value of CH_3CHO (1.167 MJ/mole, 26.49 MJ/kg) is larger than that of CH_4 (890.7 kJ/mole, 55.49 MJ/kg),[12] while the laminar burning velocities at a fuel-air equivalence ratio ϕ of 1.0 are similar (~37 cm/s for CH_3CHO,[13] ~35 cm/s for CH_4[14]). Taken with a slightly different air requirement (2.5 moles O_2 vs. 2 moles for CH_4), at low fraction in methane we expect the addition of CH_3CHO to affect the combustion properties of the fuel/air mixture in an engine cylinder (energy density, burn rate, etc.) less than an equivalent fraction of ethane, a normal minor component of natural gas. To our knowledge the ignition properties of CH_3CHO and CH_4 have not been measured under identical conditions of pressure and temperature. However, comparison of the results of Tao et al.[15] for acetaldehyde with those reported by Yu et al.[16] for methane indicates that the ignition of CH_3CHO is at least an order of magnitude faster than that of CH_4 under stoichiometric conditions. This indicates that acetaldehyde could be an effective ignition promoter.

From a mechanistic perspective, exploring the chemistry of acetaldehyde, which is an intermediate in methane oxidation, in a mixture with methane can provide insight into parts of the reaction path that may be poorly illuminated when studying the oxidation of the pure compound alone. While a number of studies have been performed for the ignition/oxidation properties of CH_3CHO,[15–19] to the authors' knowledge, no autoignition measurements or kinetic analyses have been performed for CH_4/CH_3CHO mixtures. To provide benchmark data for chemical mechanism evaluation, we report ignition delay times of CH_4/CH_3CHO mixtures measured in an RCM for a range of conditions relevant for compression-ignition engines: at ϕ of 1.0–4.0, with CH_3CHO fractions in the fuel of 0%–5%, at a pressure after compression (P_c) of roughly 60 bar and temperature after compression (T_c) between 750 and 900 K. These measurements are compared with computations using a chemical mechanism, which is a slightly modified version of that reported by Hashemi et al.[19] for acetaldehyde oxidation. We also compare the results with predictions obtained using the original mechanism from ref.[19] and that reported recently by Shrestha et al.[20] To illustrate the potential impact of CH_3CHO addition to CH_4 on ignition delay time under conditions in heavy-duty diesel engines, we simulate the ignition delay times at 100 bar as a function of temperature at low CH_3CHO fraction using the modified mechanism presented here and perform a kinetic analysis to examine the influence of CH_3CHO addition on the CH_4 oxidation process.

10974601, 2024, 9, Downloaded from https://onlinelibrary.wiley.com/doi/10.1002/kin.21727 by Danish Technical Knowledge, Wiley Online Library on [05/08/2024]. See the Terms and Conditions (https://onlinelibrary.wiley.com/terms-and-conditions) on Wiley Online Library for rules of use; OA articles are governed by the applicable Creative Commons License

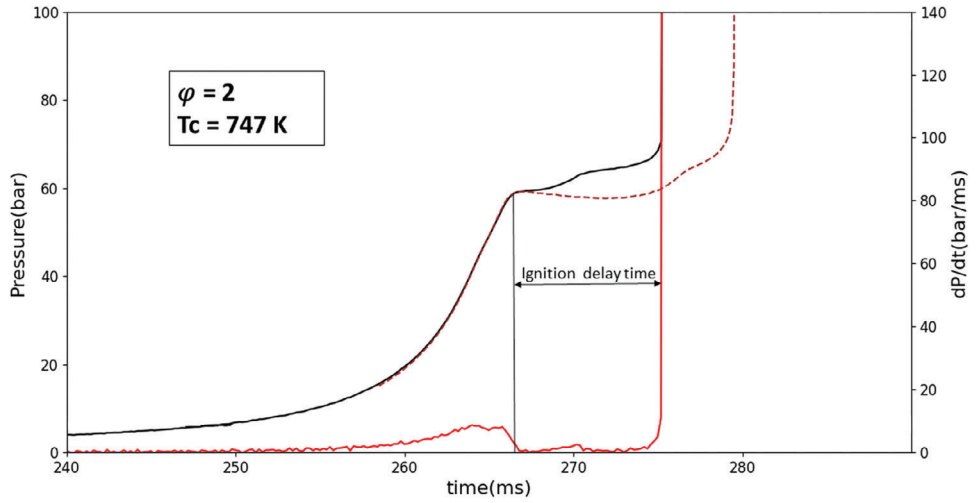

FIGURE 1 Example of pressure history for Mixture 2 (5% CH_3CHO, $\phi = 2$) at $T_c = 747$ K and $P_c = 60$ bar: measured reactive mixture (black line), dP/dt (solid red line) and simulated profile (dashed red line) using the mechanism described in Section 2.2.

TABLE 1 Compositions (mole fractions) of CH_3CHO/CH_4 mixtures.

Mixtures	Φ	X_{CH_3CHO}	X_{CH_4}	X_{O2}	X_{N2}	X_{Ar}	$\alpha = X_{CH_3CHO}/(X_{CH_4} + X_{CH_3CH})$
1	1	0.0045	0.0855	0.182	0.3	0.428	0.05
2	2	0.0083	0.1567	0.143	0.3	0.392	0.05
3	3	0.0068	0.2232	0.154	0.3	0.316	0.03
4	4	0.0057	0.2793	0.143	0.3	0.272	0.02
5	4	0.0	0.28	0.14	0.3	0.28	0

2 | EXPERIMENTS AND SIMULATIONS

2.1 | Experimental setup

The ignition delay time measurements were performed in an RCM whose details are described in refs.[7,21] Briefly, the gas mixtures were compressed in ~10–20 ms to the $P_c \sim 60$ bar, in general with 50% of the compression occurring in less than 5 ms (see Figure 1). The maximum compression ratio was 22.5, which limited the T_c that can be obtained. Consequently, to obtain different T_c after compression, the fuel/oxygen mixtures were diluted using different ratios of N_2 and Ar while keeping the total fraction (N_2 + Ar) constant. A creviced piston head was used in this machine to obtain a homogenous reacting core during the experiment.[22] A Kistler ThermoComp quartz sensor (range 1–250 bar, linearity ± 0.1%) with thermal-shock-optimized construction was installed in the bottom of the combustion chamber of RCM to monitor the pressure traces during compression and throughout the post-compression period. The pressure signal was amplified by a 5010B Kistler charge amplifier, recorded digitally by an oscilloscope with a sample rate of 500 kHz and 16-bit resolution. The compositions of the reactive mixtures examined in this study are shown in Table 1. We define the fraction of CH_3CHO in the fuel, α, as $\alpha = X_{CH_3CHO}/(X_{CH_3CHO} + X_{CH_4})$, where X_i is the mole fraction of component i. Additional experiments with pure methane as a fuel ($\alpha = 0$), conducted at $\phi = 1$–3, failed to obtain ignition.

A typical measured pressure trace for reactive Mixture 2 (Table 1) at $T_c = 747$ K is shown in Figure 1. For measurements under identical conditions (composition, initial/final pressure), the general day-to-day reproducibility of the measured ignition delay times, including repositioning of the piston height, was determined to be better than 5%, and, with the exception of the very short delay times, the uncertainty in deriving the ignition delay time from the measurements is 0.3 ms, increasing to roughly 1 ms at $\phi = 4$.

All gas mixtures were prepared in advance in a 10-L gas bottle and used to charge the RCM combustion chamber to the required initial pressure and temperature. The mixtures were allowed to mix for at least 24 h to ensure homogeneity. The T_c was calculated assuming the existence of an adiabatic core, using the standard

10974601, 2024, 9, Downloaded from https://onlinelibrary.wiley.com/doi/10.1002/kin.21727 by Danish Technical Knowledge, Wiley Online Library on [05/08/2024]. See the Terms and Conditions (https://onlinelibrary.wiley.com/terms-and-conditions) on Wiley Online Library for rules of use; OA articles are governed by the applicable Creative Commons License

thermodynamic formulation for adiabatic compression.[7,21] In general, the uncertainty of the obtained T_c is less than ±3.5 K.[23]

2.2 | Reaction mechanism

The reaction mechanism was drawn largely from Hashemi et al.[19] who studied CH_3CHO oxidation at high pressure. With the methyl radical (CH_3) being a major fuel-derived radical for both acetaldehyde and methane, most of the reactions involved in the chemical coupling between the two fuels were already included in the kinetic model from Hashemi et al. In the present work, selected subsets of the reaction mechanism were re-evaluated. Under the conditions of interest, reactions of methylperoxy (CH_3OO) and acetyldioxidanyl ($CH_3C(O)OO$) may affect ignition and chain-branching; some steps were updated according to the recent work of Cavallotti et al.[24] (see mechanism listing in Supplementary Material), but they did not show up as sensitive under the present conditions. The most important changes compared to the starting mechanism from Hashemi et al. concerned the reactions of HO_2 with itself and with methanol. The rate constant for the $HO_2 + HO_2$ reaction was updated following the recent theoretical work by Klippenstein et al.,[25] who advocated a secondary, strongly promoting product channel forming $OH + OH + O_2$. For $CH_3OH + HO_2$, the rate constant was adopted from Burke et al.,[26] following the analysis by Li et al.[27]

Table 2 lists some of the key reactions in mechanism. For most of the reactions in the acetaldehyde subset, the rate constants are similar to those preferred by Shrestha et al.[20] An exception is the $CH_3CHO + CH_3$ reaction where the rate constant for the main product channel to $CH_3CO + CH_4$ differs roughly by a factor of four; both being within the uncertainty of the available experimental results.

Regarding the predictions of the present mechanism for pure methane, we note that ignition delay times computed at high pressure are within 10% of those calculated using the mechanism for CH_4 from Hashemi et al.,[28] verified over a wide range of high-pressure conditions.

2.3 | Numerical approach

The ignition delay time is simulated using the homogenous reactor code from Cantera package.[29] We determine the ignition delay time by the interval between the end of compression and the point of maximum slope of the during the ignition of the mixture. To assess the effect of CH_3CHO fraction on the ignition behavior of CH_4, the calculations are done at constant specific volume. For comparison between measurements and numerical simulations, the varying specific volume of the RCM adiabatic core, due to the effects of compression and post-compression heat loss, is taken into account in the simulations. For this purpose, the specific volume of the adiabatic core is used as an input parameter,[30–32] which is derived from the measured pressure trace from an inert mixture. For the inert mixture, the oxygen is replaced by the inert components (N_2 and Ar), where the ratio of N_2/Ar is chosen to match the heat capacity of the reactive mixture, following Dai et al.[33] We note that several profiles showed evidence of heat release during compression, predominantly arising from the first stage in a two-stage ignition, as well as significant pre-ignition heat release for a number of mixtures. Pre-ignition heat release was also observed in NH_3/DME mixtures[34]; as done there, we continue to use the non-reactive pressure trace to derive the profile for the specific volume for these cases as well, being aware of the potential errors, as discussed in ref.[34] and references therein.

For four conditions in the measurement series of Mixture 1 (at T_c = 777, 790, 820, and 842 K), the compression was significantly slower compared to the rest of the experiments (arising from reduced pressure of the N_2 driver). This is illustrated in Figure 2. Compared to the nominal rapid compression occurring in this RCM, the relatively slow compression allowed for additional chemical reaction and heat loss during compression. Comparisons between fast compression and slow compression using inert mixtures showed a difference in P_c of 3.7 bar (at nominally 60 bar) with a maximum temperature difference at T_c of 15 K. As seen in Figure 2, the decrease in pressure after P_c is typical for "rapid" compression and indicates maintenance of the adiabatic core. Since we use the measured specific volume profile, the chemistry in the computations is constrained to follow the same pressure/temperature history as the measurements, allowing comparison of the calculated results with the experiments. As such, no exceptions have been made in the treatment of the data. The impact of any slow compression on the interpretation of the results will be discussed in Section 3.1.

Element flux analyses were performed to study the reaction paths under the experimental conditions. Sensitivity analyses were carried out to identify the most important reactions controlling the autoignition behavior. Sensitivity coefficients (S_i) were obtained using:

$$S_i = \frac{\Delta\tau/\tau}{\Delta k_i/k_i} \quad (1)$$

where $\Delta\tau$ is the change of ignition delay time corresponding to a change of rate constant Δk_i of ith reaction. A negative coefficient S indicates a promoting effect (reducing ignition delay time when a rate constant is increased) and a positive coefficient denotes an inhibiting effect

10974601, 2024, 9, Downloaded from https://onlinelibrary.wiley.com/doi/10.1002/kin.21727 by Danish Technical Knowledge, Wiley Online Library on [05/08/2024]. See the Terms and Conditions (https://onlinelibrary.wiley.com/terms-and-conditions) on Wiley Online Library for rules of use; OA articles are governed by the applicable Creative Commons License

TABLE 2 Rate coefficients of selected reactions.

Reaction	*A*	*n*	*E*	Reference
$CH_3CHO + OH = CH_3CO + H_2O$	2.6E12	0.00	−709	Hashemi et al.[19]
$CH_3CHO + OH = CH_3 + CO + H_2O$	2.5E11	0.00	−709	Hashemi et al.[19]
$CH_3CHO + OH = CH_2CHO + H_2O$	8.5E13	0.00	5313	Hashemi et al.[19]
$CH_3CHO + HO_2 = CH_3CO + H_2O_2$	1.7E13	0.00	16293	Hashemi et al.[19]
$CH_3CHO + HO_2 = CH_2CHO + H_2O_2$	1.1E13	0.00	23248	Hashemi et al.[19]
$CH_3CHO + O_2 = CH_3CO + HO_2$	1.2E05	2.50	37554	Hashemi et al.[19]
$CH_3CHO + O_2 = CH_2CHO + HO_2$	1.5E07	1.90	49548	Hashemi et al.[19]
$CH_3CHO + CH_3 = CH_2CHO + CH_4$	1.8E-1	3.44	10384	Hashemi et al.[19]
$CH_3CHO + CH_3 = CH_3CO + CH_4$	3.5E05	2.16	6234	Hashemi et al.[19]
$CH_3CHO + CH_3O = CH_3CO + CH_3OH$	2.6E04	2.58	249	Hashemi et al.[19]
$CH_3CHO + CH_3O = CH_2CHO + CH_3OH$	2.7E01	3.45	5873	Hashemi et al.[19]
Duplicate reaction	5.6E-06	4.93	628	Hashemi et al.[19]
$CH_3CHO + CH_3OO = CH_3CO + CH_3OOH$	3.2E-01	3.94	9503	Hashemi et al.[19]
Duplicate reaction	5.0E-06	4.98	5268	Hashemi et al.[19]
$CH_3CO = CH_3 + CO$	1.3E20	−2.32	18012	Hashemi et al.[19]
$CH_3OO + CH_3 = CH_3O + CH_3O$	5.1E12	0.00	−1411	Hashemi et al.[19]
$CH_3OO + CH_4 = CH_3OOH + CH_3$	4.5E-03	4.69	19868	Hashemi et al.[19]
$CH_3OO + CH_2O = CH_3OOH + HCO$	2.0E09	1.11	12500	Hashemi et al.[19]
$CH_3OO + CH_2O = CH_3OOH + H + CO$	2.5E14	0.03	30133	Hashemi et al.[19]
$CH_3OO + CH_3OO = CH_3O + CH_3O + O_2$	1.1E18	−2.40	1800	Hashemi et al.[19]
Duplicate reaction	7.0E10	0.00	800	Hashemi et al.[19]
$CH_3OH + HO_2 = CH_2OH + H_2O_2$	3.2E13	0.00	18780	Burke et al.,[26] Li et al.[27]
$CH_3OH + HO_2 = CH_3O + H_2O_2$	1.2E13	0.00	20070	Burke et al.,[26] Li et al.[27]
$HO_2 + HO_2 = H_2O_2 + O_2$	1.9E-02	4.12	−4960	Klippenstein et al.[25]
$HO_2 + HO_2 = OH + OH + O_2$	6.4E17	−1.54	8540	Klippenstein et al.[25]
$H_2O_2(+ M) = OH + OH(+ M)$	2.0E12	0.90	48749	Hashemi et al.[19]
Low pressure limit	2.5E24	−2.30	48749	Hashemi et al.[19]

The rate coefficients are in the form of $k = A\,T^n \exp(-E/(RT))$. Units are mol, cm, K, s, and cal.

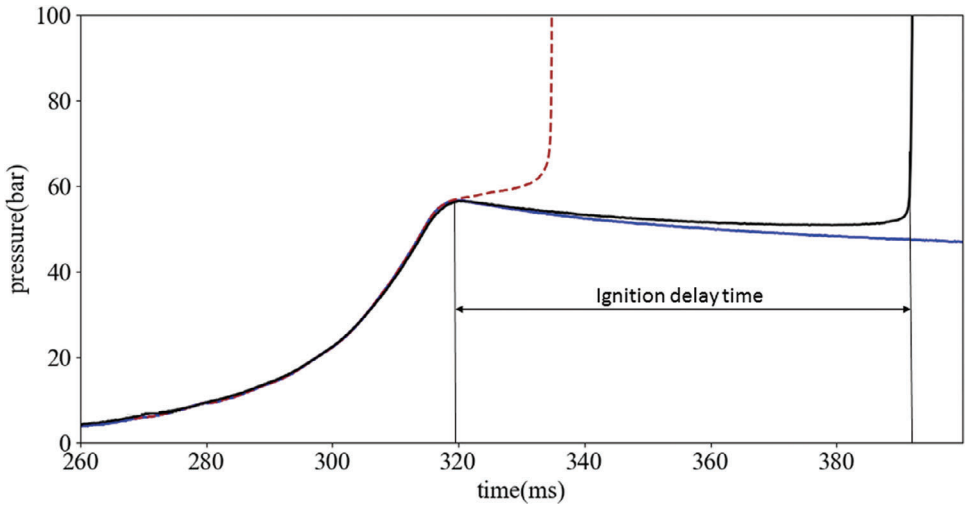

FIGURE 2 Example of pressure history for Mixture 1 at $T_c = 790$ K and $P_c = 60$ bar: measured reactive mixture (black line), the equivalent inert mixture (solid blue line), and computed profile (dashed red line).

10974601, 2024, 9, Downloaded from https://onlinelibrary.wiley.com/doi/10.1002/kin.21727 by Danish Technical Knowledge, Wiley Online Library on [05/08/2024]. See the Terms and Conditions (https://onlinelibrary.wiley.com/terms-and-conditions) on Wiley Online Library for rules of use; OA articles are governed by the applicable Creative Commons License

(increasing ignition delay time when a rate constant is increased).

3 | RESULTS AND DISCUSSION

3.1 | Characteristics of the ignition profile and experimental ignition delay times

As mentioned in section 2.1, the ignition delay time has been measured at P_c~60 bar while the T_c of the mixtures studied (Table 1) varies from 750 to 900 K. The ignition trace for $\phi = 2$ and $T_c = 747$ K (Mixture 2, $\alpha = 0.05$) in Figure 1 is typical for two-stage ignition, as also observed in NH_3/DME mixtures.[34] This assignment is aided by the dP/dt trace, with a well-defined peak from first-stage ignition appearing at ~270 ms, between that for the end of mechanical compression (~265 ms) and the sharp increase from the second stage (275 ms). In contrast, the measured pressure profile at $\phi = 1$ and $T_c = 790$ K in Figure 2 is characteristic of single-stage ignition, as expected for pure CH_4 but at a temperature at which CH_4 ignition is very slow (not measurable in the RCM). Increasing the temperature to $T_c = 831$ K at $\phi = 2$ (Figure 3A) shows a less well-defined ignition sequence than in Figure 1. Since the inert trace in Figure 3A shows compression to $P_c = 60$ bar, the results indicate significant heat release during the compression period, increasing the pressure at the end of compression by ~2 bar, as also observed in NH_3/DME mixtures.[34] While the results suggest that the first stage of ignition has been advanced into the compression period of the RCM, the pressure profile precludes identification of a clear first stage. Whereas at 790 K (Figure 2) the reactive pressure profile follows the inert profile immediately after P_c is reached, increasing the temperature at $\phi = 1$–876 K, shown in Figure 3B, results in a reactive trace that diverges from the inert trace immediately after P_c. We ascribe this phenomenon to heat release prior to ignition, albeit modest, again as reported in ref.[34]

The pressure traces at $\phi = 1$ show typical single-stage ignition at T_c below 842 K, while pre-ignition heat release is observed at higher temperatures. At $\phi = 2$ and 3, all measurements show two-stage ignition, with measurements having short ignition delay times (~1 ms) showing similar behavior to that in Figure 3A. Measurements at $\phi = 4$ show mild pre-ignition heat release, that is, with minimal pressure increase above P_c, also resembling Figure 3B at short times.

Significant heat release prior to the end of compression as illustrated in Figure 3A challenges the derivation of reliable ignition delay times from the reactive traces in these cases. To be able to extract delay times from the measurements in a reproducible fashion, we use the pressure traces from the inert mixtures. As done when comparing the measured and simulated pressure traces, we shift the time scale of the inert trace to match the reactive pressure trace. The profiles can be matched to well within 1 ms (see Figures 2 and 3), which for most cases allows obtaining ignition delay times to fractions of a ms; in Figure 4, we adapt a pro-forma uncertainty of 1 ms for the measurements at short delay times showing substantial heat release during compression. The inability to extract a clear delay time for the first stage of ignition precludes our reporting these times; consequently, we only report the overall ignition delay time below. We recommend these experiments be repeated in a facility capable of resolving ignition shorter than 1 ms, such as a shock tube, to allow a clear determination of the ignition behavior at the short times observed under these conditions.

The simulated pressure profiles for Mixture 1 ($\phi = 1.0$) exhibit the same single-stage ignition behavior as observed for the experiments, but the model predicts shorter ignition delay times: at 790 K (Figure 2) the simulation is ~20% of the measured value but improves to ~40% at 876 K (Figure 3B). We note that the computations at 790 K also significantly overpredict the pre-ignition heat release. Although at 876 K the experimental trace shows significant pre-ignition heat release, the computed pressure profile rises faster. These results indicate that the mechanism predicts the onset of chemical reactions at $\phi = 1.0$ to be earlier than observed experimentally. In this regard, we posit that the relatively slow compression for the four measurements in the range 777–842 K at $\phi = 1.0$ reported above magnifies the pre-ignition heat release, as observed in Figure 2. Slower compression allows more time for the chemistry in the computations to develop, which is already "too fast" as compared to the measurements; this then exaggerates the differences between the simulations and these experimental delay times. As mentioned in Section 3.4, constant volume simulations at $\phi = 1.0$ suggest a two-stage ignition that is not readily discernable in the experimental traces, with the first stage very close to the second ignition.

The simulations for Mixture 2 at 747 K (Figure 1) capture qualitatively the form of the two-stage ignition, but now predict ignition at longer times than observed, with the overall ignition delay time being roughly 50% longer than the measurement. At $T_c = 831$ K (Figure 3A), despite the first stage of ignition occurring during compression, the calculation for Mixture 2 qualitatively follows the experimental profile. The measured overall ignition delay time, which as described above in this section is complicated by the necessity of using the inert pressure trace to mark the end of compression, is roughly five times shorter than the computed delay time.

10974601, 2024, 9, Downloaded from https://onlinelibrary.wiley.com/doi/10.1002/kin.21727 by Danish Technical Knowledge, Wiley Online Library on [05/08/2024]. See the Terms and Conditions (https://onlinelibrary.wiley.com/terms-and-conditions) on Wiley Online Library for rules of use; OA articles are governed by the applicable Creative Commons License

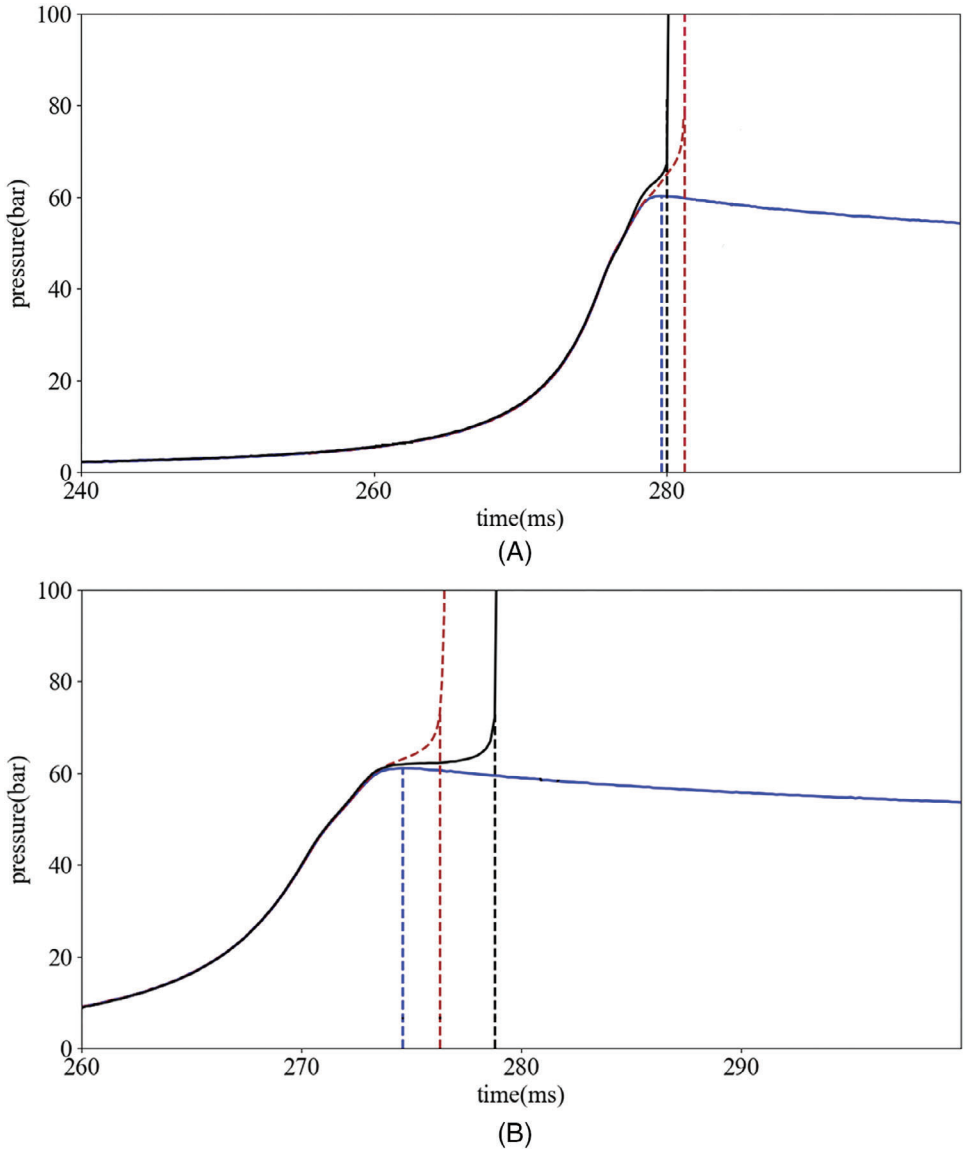

FIGURE 3 Measured pressure profiles for reactive and corresponding inert mixtures (solid black and blue lines, respectively) and simulated pressures (red dashed lines) for Mixture 2 at $T_c = 831$ K (A) and Mixture 1 at $T_c = 876$ K (B). For both mixtures, $\alpha = 0.05$.

Figure 4 shows the measured and calculated ignition delay times of the mixtures in Table 1. Calculations are conducted both with the current mechanism and those of Hashemi et al.[19] and Shrestha et al.[20] Figure 4A and B present the ignition delay time of a fuel mixture containing 5% CH_3CHO at $\phi = 1$ and 2 (Mixtures 1 and 2, respectively). The results for Mixture 3 (3% CH_3CHO at $\phi = 3.0$) are given in Figure 4C, while in Figure 4D the results for Mixture 4 (2% CH_3CHO at $\phi = 4.0$) are shown.

Due to the long ignition delay times of pure CH_4 at $\phi = 1.0$, 2.0, and 3.0, they could not be measured in the RCM in the temperature range studied. Interestingly, we could however measure the ignition delay times of pure CH_4 at $\phi = 4.0$ (Mixture 5 in Table 1) in the range 865–900 K; these data are also shown in Figure 4D. Under these conditions, addition of just 2% CH_3CHO shortens the ignition delay time by more than an order of magnitude, indicating that the efficiency of acetaldehyde as a promoter is comparable to that of other oxygenated fuels, such as alcohols and ethers.

We report that the computed delay times using the present mechanism at the highest temperatures for $\phi = 3$ and 4 were too short to be extracted reliably, even when using the inert pressure trace to determine the end of compression. Therefore, these data are not given in Figure 4C and D.

The measured ignition delay times increase monotonically with decreasing temperature, without evidence of a negative-temperature-coefficient (NTC) region under the investigated conditions. The computations show the same

10974601, 2024, 9, Downloaded from https://onlinelibrary.wiley.com/doi/10.1002/kin.21727 by Danish Technical Knowledge, Wiley Online Library on [05/08/2024]. See the Terms and Conditions (https://onlinelibrary.wiley.com/terms-and-conditions) on Wiley Online Library for rules of use; OA articles are governed by the applicable Creative Commons License

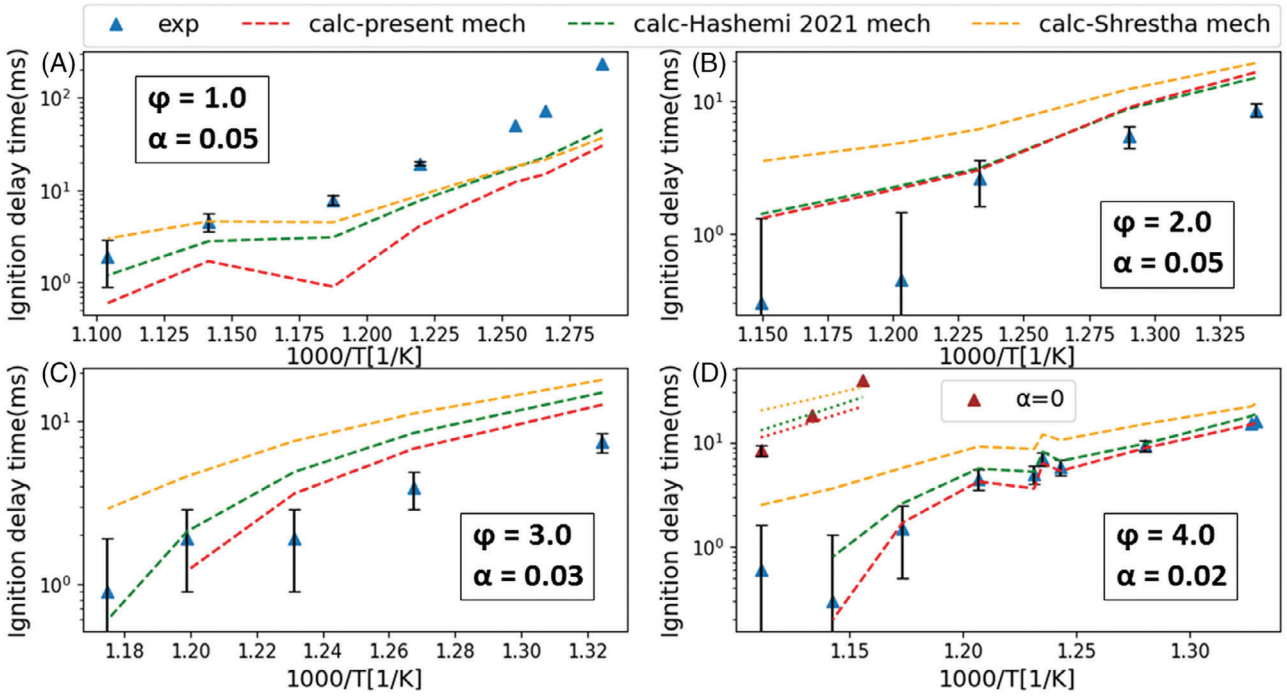

FIGURE 4 Measured and calculated ignition delay time as a function of 1000/T for the mixtures in Table 1 at ~ 60 bar, using the mechanism described here and the mechanisms from Hashemi et al.[19] and Shrestha et al.[20] The error bars of the measured ignition delay times (±5%) measurements at the lowest temperatures are covered by the symbols and therefore not visible in the figures. As discussed in the text, 1 ms error bars have been attached to the measurements at $\phi = 4$ and those with substantial heat release during compression.

behavior, with the exception of a narrow plateau in the simulations at $\phi = 1$ in the range $T = 840$–880 K, which we attribute to the accelerated ignition arising from the slow compression discussed above in this section; a plateau is not observed in the constant-volume simulations in Section 3.3. As can be seen in Figure 4A and discussed above in this section, the simulations at $\phi = 1$ tend to underpredict the ignition delay times. The discrepancy is most pronounced for the revised mechanism, while the calculations using the mechanisms of Shrestha et al.[20] and Hashemi et al.[19] bracket the measurements at the two highest temperatures. At $\phi = 2$ and 3, the computations tend to overestimate the ignition delay times, with the predictions of Shrestha et al. being somewhat higher than the other two mechanisms. While the mechanism of Hashemi et al.[19] and the present mechanism predict identical results at $\phi = 2$, the revised mechanism shows improved performance at $\phi = 3$. At $\phi = 4$, the present mechanism and that of Hashemi et al.[19] predict results that are essentially within the estimated experimental uncertainty at this equivalence ratio; here too, the simulations using Shrestha et al.[20] give slightly larger delay times. The computations generally agree with the measurements within a factor of two, with the exception of Mixture 1 where underprediction up to a factor of ~5 is observed in the temperature range 750–800 K (Figure 4A). Noteworthy is the agreement (better than a factor of ~2) observed between the measured and calculated ignition delay times of pure CH_4 at $\phi = 4$ in the temperature range of 865–900 K, with the results using the mechanism of Hashemi et al.[19] being somewhat closer to the measurements (within ~40%) than the other mechanisms. Thus, 2%–5% CH_3CHO in the fuel results in an ignitable mixture in a region of temperature and equivalence ratio for which neat CH_4 does not ignite.

3.2 | Kinetic analysis and impact of CH_3CHO addition on CH_4 oxidation

While the agreement for the total ignition delay time is within a factor of two for most of the conditions studied, for $\phi = 1$ the difference is up to a factor of five. Furthermore, the uncertainty in the prediction of the early heat release and/or the first stage of ignition limits the reliability of an analysis of the mechanism by which CH_3CHO enhances methane ignition. These discrepancies can be partly attributed to shortcomings in the peroxide chemistry[19] and more work is needed to clarify this issue. To support this goal, the identification of the major reaction paths that the current mechanism indicates and the sensitivity analysis for the total ignition delay time are performed. Following the methods described in the literature (see ref.[34] and references therein), we consider the reaction paths at 20% fuel consumption.

10974601, 2024, 9, Downloaded from https://onlinelibrary.wiley.com/doi/10.1002/kin.21727 by Danish Technical Knowledge, Wiley Online Library on [05/08/2024]. See the Terms and Conditions (https://onlinelibrary.wiley.com/terms-and-conditions) on Wiley Online Library for rules of use; OA articles are governed by the applicable Creative Commons License

3.2.1 | Temporal profiles of CH_3CHO, CH_4 and temperature

As was done in ref.,[34] insight in contributions of the two fuel components to the heat release prior to ignition can be obtained by plotting the changes in relative mole fractions of the fuels and temperature with time. Since, despite any shortcomings in the predictions of ignition delay time, the simulations using the current mechanism capture the pre-ignition temperature rise and two-stage ignition qualitatively, we use the mechanism to obtain this insight. The temperature and relative mole fractions of CH_3CHO and CH_4 derived from constant volume computations at $\alpha = 0.05$ and $T_c = 870$ K for $\phi = 1$, 2, and 4 are shown in Figure 5A, B, and C, respectively. Also following,[34] the times at which 20% of the CH_3CHO and 20% of the total fuel have been consumed are shown as well. We observe that CH_3CHO consumption begins within 1 ms for all three conditions. This is followed by a relatively constant decrease in CH_3CHO fraction, with the concomitant rise in temperature, until just prior to ignition. At 20% CH_3CHO consumption, the combustible mixture temperature has risen from 870 to 887, 893, and 898 K for $\phi = 1$, 2, and 4, respectively. We ascribe the progressive increase in temperature rise with increasing equivalence ratio to the decreasing dilution of the fuel mixture with air. At this point in the ignition process, the methane consumption is less than 1% (0.71%, 0.62%, and 0.57% at $\phi = 1$, 2, and 4, respectively) but increases steadily past this point. At 20% total fuel consumption, we observe that the CH_3CHO is nearly exhausted, with the temperature having risen to 1183, 1267, and 1371 K for $\phi = 1$, 2, and 4. It is worth contrasting this situation with the ignition of pure CH_4 under similar conditions: here, the point of 20% fuel consumption is during ignition itself, with negligible oxidation in advance of ignition. While barely discernable in Figure 5A ($\phi = 1$), both the temperature and CH_4 fraction show a change in slope very close to the time of 20% fuel consumption in Figure 5B ($\phi = 2$) and C ($\phi = 4$), indicative of the first stage of ignition, albeit only partially resolved, as discussed above.

These results indicate that CH_4 does not ignite before CH_3CHO is largely depleted. The radical pool developed in the oxidation of CH_3CHO, together with the increase in temperature, facilitates ignition. The pre-ignition heat release, which is augmented by the minor conversion of CH_4, increases the temperature to well above 1000 K, where CH_4 without the presence of an ignition enhancer in and of itself becomes short. That reactive species are predominantly responsible for the ignition enhancement observed is supported by simulations under the conditions of Figure 5A in which methane is treated as an inert species. The results show that complete oxidation of CH_3CHO raises the mixture temperature to only 908 K, indicating that heat release from CH_3CHO oxidation itself is modest in accelerating ignition.

3.2.2 | Reaction path of CH_3CHO/CH_4 mixtures

To sketch the oxidation path of the CH_4/CH_3CHO fuel mixture described by the current mechanism, the results of the carbon element flux analysis at 20% CH_3CHO consumption is shown in Figure 6 for the mixture with $\phi = 1$, $\alpha = 0.05$, $T_c = 870$ K, and $P_c = 60$ bar; these conditions correspond to those at the vertical red dashed line in Figure 5A. Fluxes lower than 5% are not shown to avoid clutter. The main reaction sequence follows that described in ref.[19] Hydrogen abstraction from CH_3CHO predominantly yields CH_3CO, which then dissociates to CH_3 and CO. Under the conditions described here, CH_3 adds to O_2 to form the CH_3OO radical. The subsequent reaction with HO_2 forms CH_3OOH, whose dissociation initiates the chain branching sequence $CH_3OOH\ (+M) \longrightarrow CH_3O + OH\ (+M)$, $CH_3O\ (+M) \longrightarrow CH_2O + H\ (+M)$, $CH_2O + OH \longrightarrow HCO + H_2O$, $HCO + O_2 \longrightarrow CO + HO_2$. The path of CH_3CHO oxidation through CH_2CHO to $CH_2O + OH + CO$ accounts for roughly 25% of the CH_3CHO flux at this stage. Interestingly, while CH_3OO was deemed unimportant in pure CH_3CHO oxidation above 800 K,[19] it is here still the dominant route for CH_3 for the conditions here (mixture temperature 884 K). In contrast to pure CH_3CHO oxidation, the formation of CH_3 is supplemented by the oxidation of CH_4 in the fuel. In addition to attack by OH, HO_2, and H, as expected for pure CH_4, there is a contribution to methane oxidation by $CH_3C(O)OO$, CH_3O, and CH_3OO, albeit for a total of ~8%. Noteworthy is that the mechanism predicts that roughly 90% of the methane oxidation at this early time in the ignition process is caused by OH, presumably produced by the dissociation of CH_3OOH. However, the CH_4 consumption is limited in the presence of CH_3CHO, because a significant fraction of the CH_3 is recycled to CH_4 through the reaction $CH_3CHO + CH_3 \longrightarrow CH_3CO + CH_4$. We note in passing that performing the same analysis at $\phi = 3$, $\alpha = 0.07$, $T_c = 870$ K, and $P_c = 60$ bar shows essentially the same path as shown in Figure 6 at 20% CH_3CHO oxidation. These results indicate that the reactive species, particularly OH, produced during the oxidation of CH_3CHO assist in the decomposition of the CH_4.

We now consider the path at the time of 20% total fuel consumption at $\phi = 1.0$, shown in Figure 7; the conditions are those extant at the vertical blue dashed line in Figure 4A. Methane is again attacked predominantly by OH, with smaller contributions from H, HO_2, O_2, and O.

10974601, 2024, 9, Downloaded from https://onlinelibrary.wiley.com/doi/10.1002/kin.21727 by Danish Technical Knowledge, Wiley Online Library on [05/08/2024]. See the Terms and Conditions (https://onlinelibrary.wiley.com/terms-and-conditions) on Wiley Online Library for rules of use; OA articles are governed by the applicable Creative Commons License

INTERNATIONAL JOURNAL OF CHEMICAL KINETICS

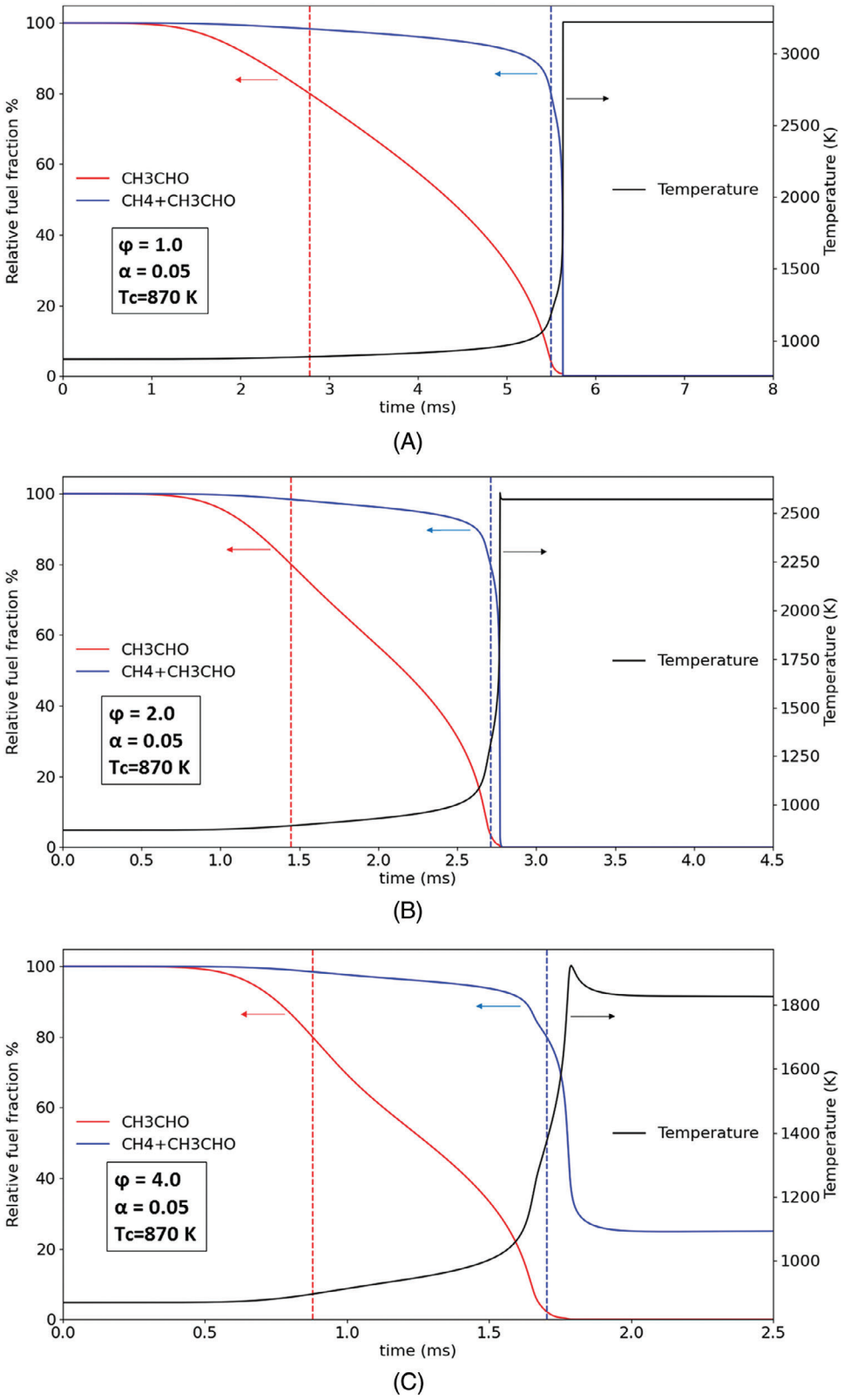

FIGURE 5 Computed profiles of mixture temperature and normalized mole fractions of CH_3CHO (solid red curve) and CH_4 at (solid blue curve) $\alpha = 0.05$ and $T_c = 870$ K for $\phi = 1$ (A), 2 (B), and 4 (C). Vertical dashed lines indicate the points at which 20% CH_3CHO (red) and 20% total fuel (blue) has been consumed.

10974601, 2024, 9, Downloaded from https://onlinelibrary.wiley.com/doi/10.1002/kin.21727 by Danish Technical Knowledge, Wiley Online Library on [05/08/2024]. See the Terms and Conditions (https://onlinelibrary.wiley.com/terms-and-conditions) on Wiley Online Library for rules of use; OA articles are governed by the applicable Creative Commons License

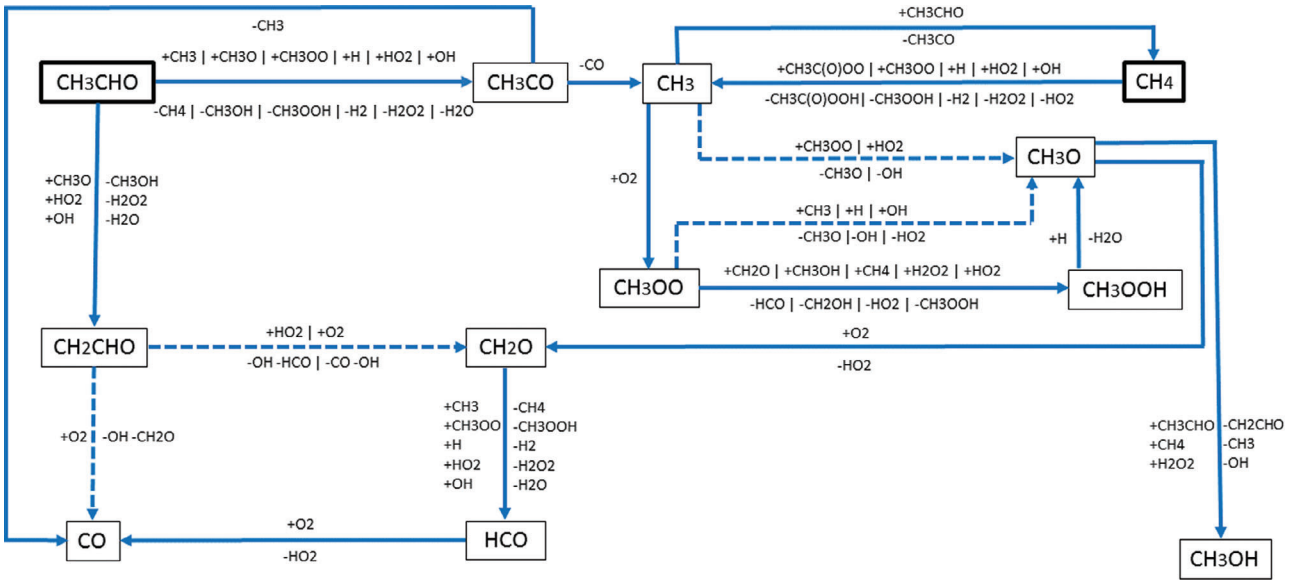

FIGURE 6 Carbon element flux analysis of CH_4/CH_3CHO fuel mixture at $\alpha = 0.05$, $\phi = 1.0$, $T_c = 870$ K, and $P_c = 60$ bar and at the moment of 20% CH_3CHO consumption. The arrows show the direction of the reactions, while solid lines present primary paths and dashed lines denote minor paths.

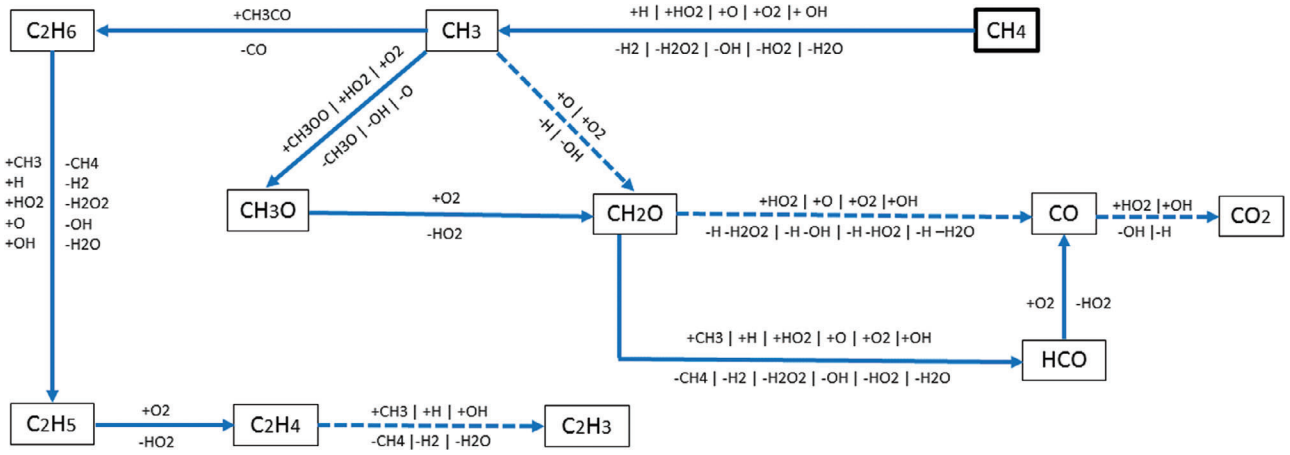

FIGURE 7 Carbon element flux analysis of CH_4/CH_3CHO fuel mixture at $\alpha = 0.05$, $\phi = 1.0$, $T_c = 870$ K, and $P_c = 60$ bar and at the moment of 20% total fuel consumption. The arrows show the direction of the reactions, while solid lines present primary paths and dashed lines denote minor paths.

Since CH_3CHO is at this time essentially depleted, intermediates in its oxidation show no contribution in the oxidation of methane. Now, CH_3 reacts in roughly equal fractions with (mainly) HO_2 to form CH_3O or with CH_3 to form C_2H_6. To a lesser extent, CH_3 reacts with O_2 to form CH_2O directly. At this time and temperature (1183 K), C_2H_6 reacts partially along the C_2 chain, with the $C_2H_3 + O_2$ reaction feeding back into C_1-species. We note further that the path shows only modest differences with that of pure CH_4 at $\phi = 1.0$, $T_c = 870$ K, and $P_c = 60$ bar and 20% fuel consumption. At $\phi = 3.0$, $\alpha = 0.07$, $T_c = 870$ K, and $P_c = 60$ bar and 20% fuel consumption, most of the CH_3 is converted via the C_2 path with a significant contribution from the reaction with OH to form methanol. For pure CH_4 under the same conditions, we observe a complete conversion via C_2 species, without any formation of methanol at the time of 20% fuel conversion.

3.2.3 | Sensitivity analysis for CH_3CHO/CH_4 mixtures

To assess the impact of CH_3CHO on CH_4 ignition, Figure 8 shows the results of sensitivity analyses using the cur-

10974601, 2024, 9, Downloaded from https://onlinelibrary.wiley.com/doi/10.1002/kin.21727 by Danish Technical Knowledge, Wiley Online Library on [05/08/2024]. See the Terms and Conditions (https://onlinelibrary.wiley.com/terms-and-conditions) on Wiley Online Library for rules of use; OA articles are governed by the applicable Creative Commons License

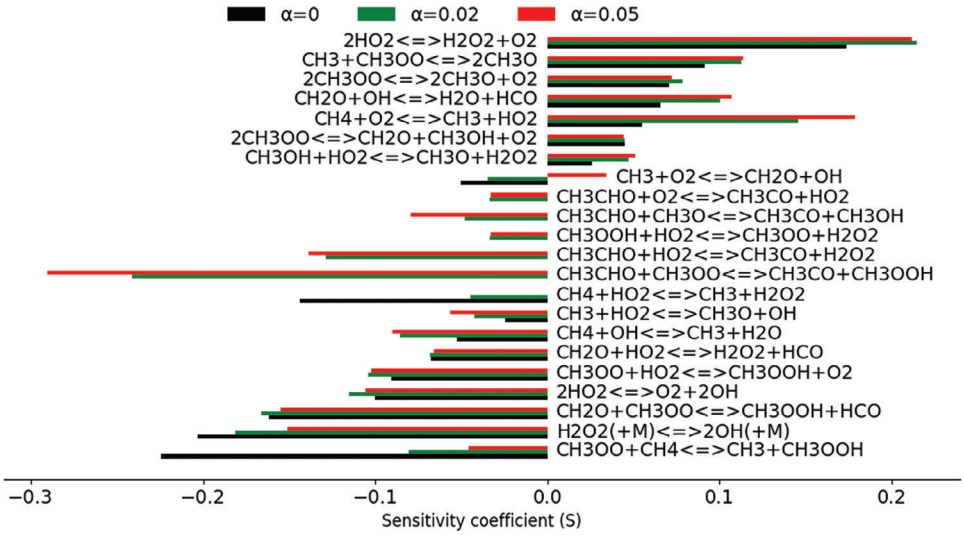

FIGURE 8 Sensitivity analysis for the ignition delay time of the fuel mixture with $\alpha = 0$, 0.02, and 0.05 at $\phi = 1.0$, $T_c = 870$ K, and $P_c = 60$ bar.

rent mechanism for mixtures with $\alpha = 0$, 0.02, and 0.05 at $\phi = 1.0$, $T_c = 870$ K, and $P_c = 60$ bar. The sensitivity analysis of pure CH_4 ($\alpha = 0$) shows reactions identified previously[28] (for $\phi = 0.5$, $T_c = 1010$ K), with important enhancing reactions such as those of CH_4 and CH_3 with HO_2 and hydrogen abstraction from CH_4 by CH_3OO. However, we observe a number of differences with the analysis in ref.,[28] which we ascribe to the lower temperature considered here (870 vs. 1010 K in ref.[28]). Noteworthy is the absence of $H + O_2 = OH + H$ in Figure 8 and the appearance of the dissociation of H_2O_2 as a dominant ignition-enhancing reaction for pure methane, which shows only minor sensitivity in the analysis in ref.[28] Also, the reaction $2HO_2 = O_2 + 2OH$ appears as a significant ignition-enhancing counterpart to $2HO_2 = H_2O_2 + O_2$.

Upon addition of CH_3CHO at $\alpha = 0.02$ and 0.05, five new ignition-promoting reactions appear in the sensitivity analysis: $CH_3CHO + CH_3OO = CH_3CO + CH_3OOH$, $CH_3CHO + HO_2 = CH_3CO + H_2O_2$, $CH_3OO + HO_2 = CH_3OOH + O_2$, $CH_3CHO + CH_3O = CH_3CO + CH_3OH$, and $CH_3CHO + O_2 = CH_3CO + HO_2$. While four of these reactions initiate the decomposition of the fuel, $CH_3CHO + CH_3OO$ becomes the most important reaction at both acetaldehyde fractions. We attribute the importance of this reaction (and that of $CH_3OO + HO_2$) to the production of CH_3OOH, which initiates chain branching with concomitant OH formation used to decompose CH_4 as discussed above. We also note that $CH_3CHO + CH_3OO$ strongly enhanced oxidation in the flow reactor experiments on pure acetaldehyde.[19] In addition, we observe the substantially increased sensitivity of ignition to $CH_3 + HO_2 = CH_4 + O_2$ and $CH_4 + OH = CH_3 + H_2O$. Interesting to note is that $CH_4 + HO_2 = CH_3 + H_2O_2$ no longer enhances ignition at 5% CH_3CHO, while the sensitivity of ignition to $CH_3OO + CH_4 = CH_3 + CH_3OOH$, which together with the dissociation of H_2O_2 is the one of the strongest ignition-enhancing reactions in pure CH_4, is decreased by a factor of 4. Further, although $CH_3 + O_2$ has a relatively modest net impact on ignition, it changes from ignition enhancing at $\alpha = 0$ and 0.02 to ignition inhibiting at 5% acetaldehyde in the fuel.

We compare the effect of equivalence ratio on the sensitivity of ignition at 5% acetaldehyde in the fuel at $T_c = 870$ K, and $P_c = 60$ bar for $\phi = 1$, 2, and 4 in Figure 9. Here we see that, in general, the equivalence ratio has only a modest influence on the sensitivities at fixed CH_3CHO fraction in the fuel. Exceptions that only appear in the fuel-rich mixtures are the recombination of CH_3 (inhibiting) and $CH_3C(O)OO + CH_4 = CH_3 + CH_3C(O)OO$ (enhancing). In addition, there are two reactions that show sensitivity at $\phi = 1$ and 2, but not at $\phi = 4$: $2CH_3OO = 2CH_3O + O_2$, which inhibits ignition presumably by bypassing the chain-branching sequence initiated by CH_3OOH, and the enhancing reaction $CH_3CHO + OH = CH_2CHO + H_2O$.

3.3 | Exploratory simulations of ignition in CH_4/CH_3CHO mixtures

With an eye toward using acetaldehyde as an ignition-enhancing additive in compression-ignition engines, we briefly explore the enhancement that can be achieved for pressures and temperatures extant in heavy-duty diesel engines, that is, $P_c = 100$ bar. The simulations of the ignition process in CH_4/CH_3CHO fuel mixtures are performed

10974601, 2024, 9, Downloaded from https://onlinelibrary.wiley.com/doi/10.1002/kin.21727 by Danish Technical Knowledge, Wiley Online Library on [05/08/2024]. See the Terms and Conditions (https://onlinelibrary.wiley.com/terms-and-conditions) on Wiley Online Library for rules of use; OA articles are governed by the applicable Creative Commons License

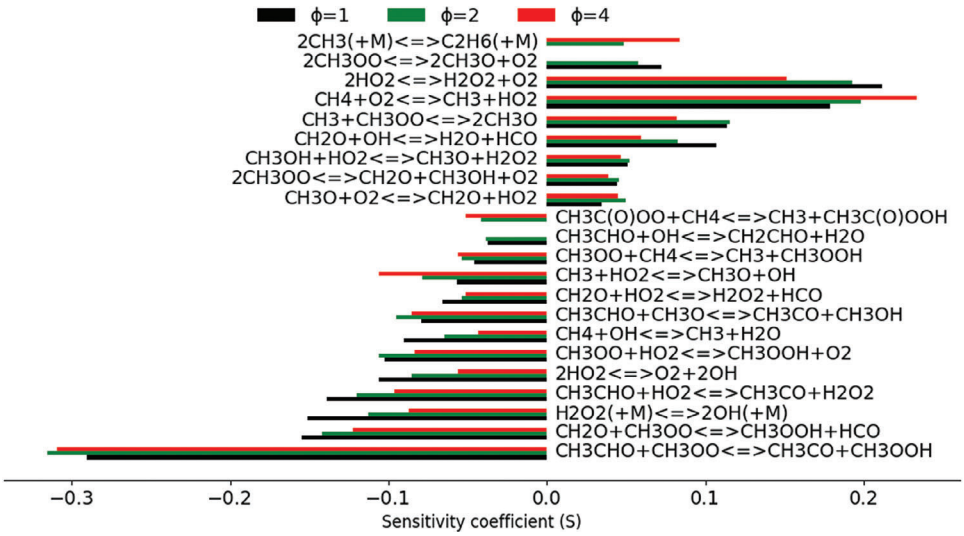

FIGURE 9 Sensitivity analysis for the ignition delay time of the fuel mixture with $\alpha = 0.05$ at $\phi = 1$, 2, and 4, $T_c = 870$ K, and $P_c = 60$ bar.

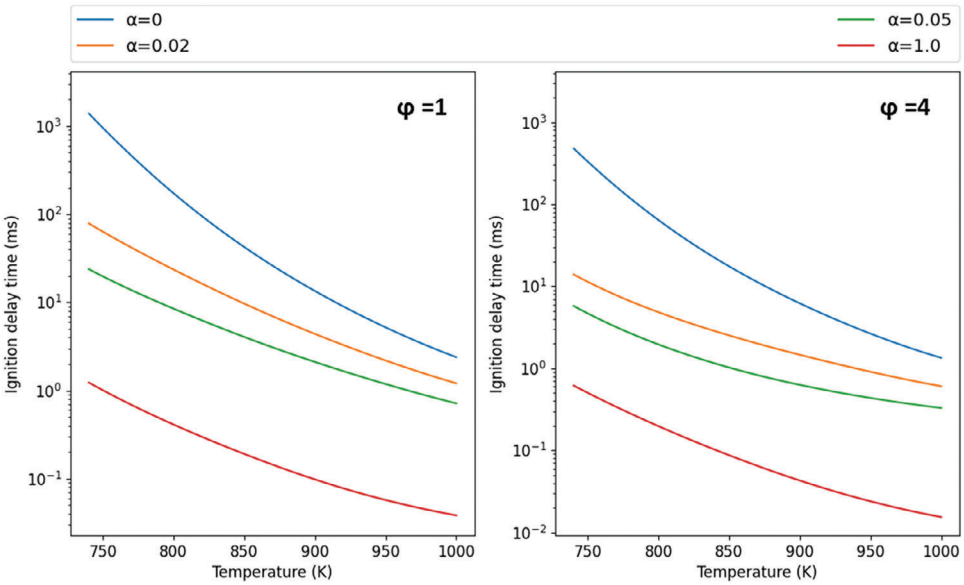

FIGURE 10 Ignition delay time as a function of temperature at $\phi = 1.0$ and 4.0 for the fuel with $\alpha = 0$, 0.02, 0.05, and 1. $P_c = 100$ bar.

using the mechanism described here by assuming a constant specific volume, that is, no heat loss. The composition of the oxidizer is fixed and close to that used in the experiments at $\phi = 1$ (see Table 1), which, for convenience, we take as $20\%O_2 + 33\%N_2 + 47\%Ar$.

To illustrate the variation in ignitability in different parts of a fuel jet mixing in hot compressed air in an engine cylinder, in Figure 10 we show the temperature dependence of the ignition delay time at $\phi = 1$ and 4, for T_c varying from 750 to 1000 K at $\alpha = 0$, 0.02, 0.05, and noteworthy is that the ignition delay time for all mixtures decreases monotonically with T_c in this range of temperature, that is, without noticeable NTC behavior. As can be seen, the ignition delay time has strong initial dependence upon α. Addition of 5% CH_3CHO to CH_4 reduces the ignition delay time by almost an order of magnitude for both ϕ. Interesting is the observation that the decrease in ignition delay time with T_c is less steep at $\alpha = 0.02$ and 0.05 than for the pure fuels. As seen at $\phi = 1$ (Figure 10A), increasing α from 0 to 0.02 reduces ignition delay time from almost 2 orders of magnitude at $T_c = 750$ K but by less than a factor of 2 at 1000 K. Similar behavior is also observed at $\phi = 4$ (Figure 10B). Figure 10A shows that, at $\phi = 1$, 5% CH_3CHO results in an ignition delay time of ~10 ms at a T_c of just below 900 K, as compared to ~1000 K for pure methane. We note that this reduction in the temperature required to achieve the same

10974601, 2024, 9, Downloaded from https://onlinelibrary.wiley.com/doi/10.1002/kin.21727 by Danish Technical Knowledge, Wiley Online Library on [05/08/2024]. See the Terms and Conditions (https://onlinelibrary.wiley.com/terms-and-conditions) on Wiley Online Library for rules of use; OA articles are governed by the applicable Creative Commons License

delay time is substantially lower than that observed for similar fractions of DME in NH_3.[34] Increasing the equivalence ratio to 4 (Figure 10B) decreases the T_c needed for a 10 ms delay time from 950 to 750 K.

4 | CONCLUSIONS

The effect of small fractions (2–5 mole%) of CH_3CHO on the ignition delay time of CH_4 in stoichiometric and fuel-rich mixtures ($\phi = 1$–4) have been examined at high pressure (60 bar) in an RCM at temperatures after compression of ~750–900 K. The results indicate that CH_3CHO has a strong ignition-enhancing effect on CH_4, with small fractions permitting ignition at temperatures where CH_4 itself does not ignite experimentally. The efficiency of acetaldehyde as a promoter is comparable to that of other oxygenated fuels like alcohols and ethers. The mixtures of CH_3CHO and CH_4 show complex ignition profiles, varying from pre-ignition heat release and/or unresolved two-stage ignition to clear two-stage ignition. Due to these complexities, further experimental study at shorter time resolution, for example, in a shock tube, is recommended. Simulation of the experimental profiles using a modified mechanism for CH_3CHO oxidation captured the shapes of the temporal profiles. Except at stoichiometric conditions, the simulated total ignition delay times were within a factor of 2 of the measurements. At $\phi = 1$, the computed delay times were significantly shorter than those measured, while at $\phi = 2$ and 3, the computations overpredicted the results. At $\phi = 4$, the simulations were within the experimental uncertainty for CH_3CHO/CH_4 mixtures and within a factor of 2 of the experimental results for pure CH_4.

The calculations indicate that CH_3CHO is nearly exhausted before the CH_4 has been consumed by 20% for all equivalence ratios studied, partly due to recycling of CH_3 to CH_4 by reaction with CH_3CHO. Analysis of the mechanism indicates that low-temperature chain-branching reactions of CH_3CHO are responsible for the acetaldehyde consumption, generating radicals that initiate the decomposition of CH_4. The heat generated by this relatively slow process raises the pre-ignition temperature of the mixture substantially, facilitating ignition. Sensitivity analysis shows that, even at low additive fractions, reactions involved in the decomposition of CH_3CHO dominate the sensitivity.

ACKNOWLEDGMENTS

The authors would like to express their thanks to H. Darmeveil from DNV, L. Dai, and J. Haak from University of Groningen, The Netherlands.

CONFLICT OF INTEREST STATEMENT

The authors declare that they have no known competing financial interests or personal relationships that could have appeared to influence the work reported in this paper.

DATA AVAILABILITY STATEMENT

Data will be made available on request.

REFERENCES

1. Molino A, Nanna F, Ding Y, Bikson B, Braccio G. Biomethane production by anaerobic digestion of organic waste. *Fuel*. 2013;103:1003-1009.
2. Korakianitis T, Namasivayam AM, Crookes RJ. Natural-gas fueled spark-ig- nition (SI) and compression-ignition (CI) engine performance and emissions. *Prog Energy Combust Sci*. 2011;37:89-112.
3. Kofod M, Sleeswijk Visser F, Bosma P, et al. LNG fuel differentiation: dME/LNG blends for HPDI engines. *SAE Int J Adv Curr Pract Mobil*. 2021;3:287-298.
4. Burke U, Somers KP, O'Toole P, et al. An ignition delay and kinetic modeling study of methane, dimethyl ether, and their mixtures at high pressures. *Combust Flame*. 2015;162(2):315-330.
5. Zhu J, Li J, Wang S, Raza M, et al. Ignition delay time measurements and kinetic modeling of methane/diesel mixtures at elevated pressures Ignition delay time measurements and kinetic modeling of methane/diesel mixtures at elevated pressures. *Combust Flame*. 2021;229:111390.
6. Gersen S, Anikin NB, Mokhov AV, Levinsky HB. Ignition properties of methane/hydrogen mixtures in a rapid compression machine. *Int J Hydrog Energy*. 2008;33:1957-1964.
7. Gersen S, Mokhov AV, Darmeveil JH, Levinsky HB, Glarborg P. Ignition-promoting effect of NO2 on methane, ethane and methane/ethane mixtures in a rapid compression machine. *Proc Combust Inst*. 2011;33(1):433-440.
8. Jouzdani S, Zheng X, Coombs DM, Akih-Kumgeh B. Experimental study of methane and methyl propanoate high-temperature kinetics. *Energy Fuels*. 2018;32(11):11864-11875.
9. Zheng X, Jouzdani S, Akih-Kumgeh B. Auto ignition study of methane and bio alcohol fuel blends. *J Eng Gas Turbine Power*. 2019;141(12):121015.
10. Huang J, Bushe WK, Hill PG, Munshi SR. Experimental and kinetic study of shock initiated ignition in homogeneous methane–hydrogen–air mixtures at engine-relevant conditions. *Int J Chem Kinet*. 2006;38:221-233.
11. Abdulrazzaq HT, Schwartz TJ. *Catalytic Conversion of Ethanol to Commodity and Specialty Chemicals*. Elsevier Inc.; 2019.
12. Malcolm J, Chase W. *NIST-JANAF Thermochemical Tables*. American Institute of Physics for the National Institute of Standards and Technology; 1998.
13. Christensen M, Abebe MT, Nilsson EJK, Konnov AA. Kinetics of premixed acetaldehyde + air flames. *Proc Combust Inst*. 2015;35(1):499-506.
14. Egolfopoulos FN, Zhu DL, Law CK. Experimental and numerical determination of laminar flame speeds: mixtures of C2-hydrocarbons with oxygen and nitrogen. *Symp (Int) Combust*. 1991;23(1):471-478.

10974601, 2024, 9, Downloaded from https://onlinelibrary.wiley.com/doi/10.1002/kin.21727 by Danish Technical Knowledge, Wiley Online Library on [05/08/2024]. See the Terms and Conditions (https://onlinelibrary.wiley.com/terms-and-conditions) on Wiley Online Library for rules of use; OA articles are governed by the applicable Creative Commons License

15. Tao T, Kang S, Sun W, et al. A further experimental and modeling study of acetaldehyde combustion kinetics. *Combust Flame*. 2018;196:337-350.
16. Yu Y, Vanhove G, Griffiths JF, De Ferrières S, Pauwels JF. Influence of EGR and syngas components on the autoignition of natural gas in a rapid compression machine: a detailed experimental study. *Energy Fuels*. 2013;27:3988-3996.
17. Won S, Ryu J, Bae J, Kim Y, Kang J. Shock-tube study of the oxidation of acetaldehyde at high temperature. *Bull Korean Chem Soc*. 2000;21:487-492.
18. Dagaut P, Reuillon M, Voisin D, Cathonnet M, Mcguinness M, Simmie JM. Acetaldehyde oxidation in a JSR and ignition in shock waves : experimental and comprehensive kinetic modeling. *Combust Sci Technol*. 2007;107:301-316.
19. Hashemi H, Christensen JM, Marshall P, Glarborg P. Acetaldehyde oxidation at elevated pressure. *Proc Combust Inst*. 2021;38(1):269-278.
20. Shrestha KP, Giri BR, Adil M, et al. Detailed chemical kinetic study of acetaldehyde oxidation and its interaction with NOx. *Energy Fuels*. 2021;35:14963-14983.
21. Gersen S, Mokhov AV, Darmeveil JH, Levinsky HB. Ignition properties of n-butane and iso-butane in a rapid compression machine. *Combust Flame*. 2010;157:240-245.
22. Park P, Keck JC. Rapid compression machine measurements of ignition delays for primary reference fuels. *SAE Trans*. 1990;99:11-23.
23. Gersen S. Experimental Study of the Combustion Properties of Methane/Hydrogen Mixtures. Ph.D. Thesis. University of Groningen; 2007.
24. Cavallotti C, Pelucchi M, Frassoldati A. Analysis of acetic acid gas phase reactivity: rate constant estimation and kinetic simulations. *Proc Combust Inst*. 2019;37:539-546.
25. Klippenstein SJ, Sivaramakrishnan R, Burke U, et al. HO2 +HO2: high level theory and the role of singlet channels. *Combust Flame*. 2022;243:111975.
26. Burke U, Metcalfe WK, Burke SM, Heufer KA, Daguat P, Curran HJ. A detailed chemical kinetic modeling, ignition delay time, and jet-stirred reactor study of methanol oxidation. *Combust Flame*. 2016;165:125-136.
27. Li G, Hashemi H, Glarborg P, Lu Y. A kinetic model for high-pressure methanol oxidation in gas phase and supercritical water. *Energy Fuels*. 2022;36:575-588.
28. Hashemi H, Christensen JM, Gersen S, Levinsky HB, Klippenstein SJ, Glarborg P. High-pressure oxidation of methane. *Combust Flame*. 2016;172:349-364.
29. Goodwin DG, Moffat HK, Schoegl I, Speth RL, Weber BW. Cantera: An object-oriented software toolkit for chemical kinetics, thermodynamics, and transport processes. https://www.cantera.org, 2023. Version 3.0.0. doi:10.5281/zenodo.8137090.
30. Mittal G, Sung CJ, Yetter RA. Autoignition of H2/CO at elevated pressures in a rapid compression machine. *Int J Chem Kinet*. 2006;38(8):516-529.
31. Lee D, Hochgreb S. Rapid compression machines: heat transfer and suppression of corner vortex. *Combust Flame*. 1998;114:531-545.
32. Tanaka S, Ayala F, Keck JC. A reduced chemical kinetic model for HCCI combustion of primary reference fuels in a rapid compression machine. *Combust Flame*. 2003;133(4):467-481.
33. Dai L, Gersen S, Glarborg P, Levinsky HB, Mokhov AV. Experimental and numerical analysis of the autoignition behavior of NH3 and NH3/H2 mixtures at high pressure. *Combust Flame*. 2020;215:134-144.
34. Dai L, Hashemi H, Glarborg P, Gersen S, Marshall P. Ignition delay times of NH3/DME blends at high pressure and low DME fraction : rCM experiments and simulations. *Combust Flame*. 2021;227:120-134.

How to cite this article: Najafi SBN, Gersen S, Hashemi H, Glarborg P, Mokhov AV, Levinsky HB. Autoignition enhancement of methane by admixture of low fraction of acetaldehyde: Simulations and RCM experiments in stoichiometric and rich mixtures. *Int J Chem Kinet*. 2024;56:534–548. https://doi.org/10.1002/kin.21727

10974601, 2024, 9, Downloaded from https://onlinelibrary.wiley.com/doi/10.1002/kin.21727 by Danish Technical Knowledge, Wiley Online Library on [05/08/2024]. See the Terms and Conditions (https://onlinelibrary.wiley.com/terms-and-conditions) on Wiley Online Library for rules of use; OA articles are governed by the applicable Creative Commons License